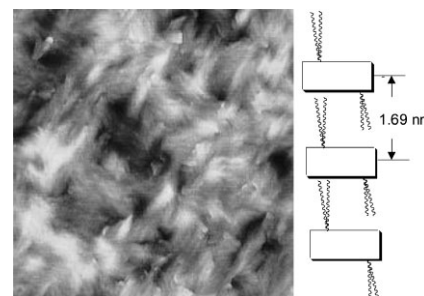


# Phase Transition Behavior and Molecular Orientation of Oligo(9,9'-dioctylfluorene-*alt*-bithiophene)

Na Li, Xiaojie Zhang, Yanhou Geng, Zhaohui Su\*

A novel conjugated oligomer, oligo(9,9'-dioctylfluorene-*alt*-bithiophene) (OF8T2), was found to exhibit a unique phase transition between crystalline and liquid-crystalline states, and a liquid-crystalline glass was easily generated, offering better TFT device performance. In thin films, upon annealing the OF8T2 molecules oriented preferentially with their planes of conjugation being normal to the substrate, and both film thickness and annealing temperature were critical to the film morphology and the molecular orientation. When the OF8T2 film was deposited on a rubbed polyimide surface and annealed, the molecules aligned their long axes along the rubbing direction.



## Introduction

Conjugated oligomers and polymers have attracted extensive interest in recent years due to their excellent semiconducting and photophysical properties, which make them promising candidates for electronic and photonic devices such as thin-film transistors (TFTs),<sup>[1–3]</sup> organic solar cells,<sup>[4]</sup> and light-emitting diodes (LEDs).<sup>[5,6]</sup> Among them, poly(fluorene-*co*-bithiophene) has proved to be one of the most promising semiconducting polymers because it combines the advantages of both fluorene and bithiophene. It exhibits relatively high photoluminescence and good stability to atmospheric oxygen as well as desired charge transport capability.<sup>[7,8]</sup> On the other hand, in devices film morphology and ordered structures are critical factors in addition to molecular structure of the material in determining device performance, and molec-

ular orientation correlates strongly with their excellent device properties. For example, field-effect transistors using P3HT as the active layer exhibited high mobility of up to  $0.1 \text{ cm}^2 \cdot \text{V}^{-1} \cdot \text{s}^{-1}$  with the edge-on orientation of the chains,<sup>[9–13]</sup> while the mobility with face-on chain orientation was 100 times lower.<sup>[12]</sup> Therefore, it is essential to explore molecular orientation in thin films of conjugated polymers. To date, many efforts have been devoted to the understanding and manipulation of polymer packing behavior in thin films, and a valuable way to align the conjugated molecules in thin films is to take advantage of the self-organization nature of liquid crystals. In other words, hairy-rod conjugated molecules which show nematic liquid-crystalline behavior offer an important way to control the desired microstructure.<sup>[14]</sup> For example, enhanced charge carrier mobility has been reported for poly(9,9'-dioctylfluorene-*alt*-bithiophene) (PF8T2), a hairy-rod polymer, in the liquid-crystalline phase after annealing on a rubbed polyimide surface.<sup>[15–17]</sup>

Compared with polymers, monodisperse oligomers have well-defined and uniform structures with few defects, and thus permit systematic investigation of structure–property relationships. Although PF8T2 has been studied in detail, reports on understanding and

N. Li, X. Zhang, Y. Geng, Z. Su  
State Key Laboratory of Polymer Physics and Chemistry,  
Changchun Institute of Applied Chemistry, Graduate School of  
the Chinese Academy of Sciences, Chinese Academy of Sciences,  
Changchun 130022, China  
Fax: +86 431 8526 2126; E-mail: zhsu@ciac.jl.cn

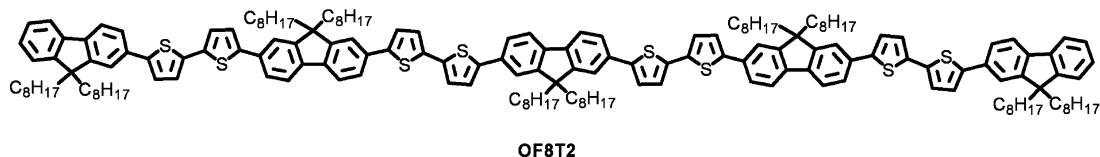


Figure 1. Chemical structure of OF8T2.

controlling molecular orientation in thin films of corresponding oligomers are very limited, and in particular liquid-crystalline oligomers of similar structure have hardly been studied. Recently, we synthesized a series of monodisperse oligo(fluorene-*co*-bithiophene)s and studied their adsorption and photoluminescence properties.<sup>[18]</sup> In the current paper, oligo(9,9'-dioctylfluorene-*alt*-bithiophene) (OF8T2, as shown in Figure 1), was chosen as a model for the investigation of the phase transitions of the conjugated oligomer in the bulk, as well as film morphology and molecular orientation in thin films, and it was found that both film thickness and annealing temperature were critical to the formation of ordered structure in the films.

## Experimental Part

### Materials

The oligomer structure is shown in Figure 1. The molecular weight of the OF8T2 was 2602.14, and its polydispersity index (PDI) was 1.03.

### Substrate Preparation

Silicon wafer, cover glass plate, and quartz wafer were used as substrates. All the substrates were first cleaned in a piranha solution [ $\text{H}_2\text{SO}_4/30\% \text{H}_2\text{O}_2$  70:30 v/v] at 80 °C for 2 h, and then removed and thoroughly rinsed with Milli-Q water ( $18.2 \text{ M}\Omega \cdot \text{cm}^2$ ), and dried in a stream of nitrogen prior to use.

### Film Preparation

Films of different thicknesses were fabricated by spin-coating OF8T2 chloroform solutions of various concentrations (0.25 to 1.0 wt.-% at 2000 rpm for 30 s. The films were placed under vacuum for 3 h to remove residual solvent.

### Measurements

Thermal properties of the oligomer were measured on a TA 2920 differential scanning calorimeter at a scanning rate of  $10 \text{ }^\circ\text{C} \cdot \text{min}^{-1}$ . UV-vis absorption spectra of the oligomer in chloroform solution and in film were collected on a Shimadzu UV-2450 spectrophotometer. Wide angle X-ray diffraction (WAXD) measurements were carried out on a D/max 2500PC diffractometer equipped with a Rigaku 18 KW rotating-anode generator

(Cu  $K_\alpha$ ) operating at 50 KV and 250 mA with a scanning rate of  $2 \text{ }^\circ\text{C} \cdot \text{min}^{-1}$ . For in situ WAXD experiments, the samples were heated at a rate of  $10 \text{ }^\circ\text{C} \cdot \text{min}^{-1}$ , and in situ WAXD patterns were collected at the desired temperatures. A Leica polarized optical microscope equipped with a Linkam TMS-94 hot stage was employed for morphology observations. Tapping-mode atomic force microscopy (AFM) was performed on a Seiko SPA-300HV scanning probe microscope with an SPI 3800N controller. Etched silicon cantilevers with a spring constant of  $42 \text{ N} \cdot \text{m}^{-1}$  were used.

## Results and Discussion

### Phase Transition Behavior

Before studying thin film morphology and molecular orientation, it is important to identify the phase transitions of the oligomer in the bulk. Differential scanning calorimetry (DSC) and polarized optical microscopy (POM) were employed to investigate the phase transitions. The OF8T2 sample was first heated to 200 °C in the DSC to eliminate the thermal history, and the first cooling and the second heating curves at a scanning rate of  $10 \text{ }^\circ\text{C} \cdot \text{min}^{-1}$  in  $\text{N}_2$  atmosphere are shown in Figure 2. It can be seen that OF8T2 exhibits two endothermic peaks at 157 and 179 °C, and a glass transition at 65 °C. The first peak at 157 °C is attributed to the crystalline-to-liquid crystalline phase transition ( $T_m$ ). In comparison, it has been reported that PF8T2, the polymer with the same repeat unit as OF8T2, shows two peaks for the crystalline/liquid crystalline transition, which are due to the complexity of melting in a

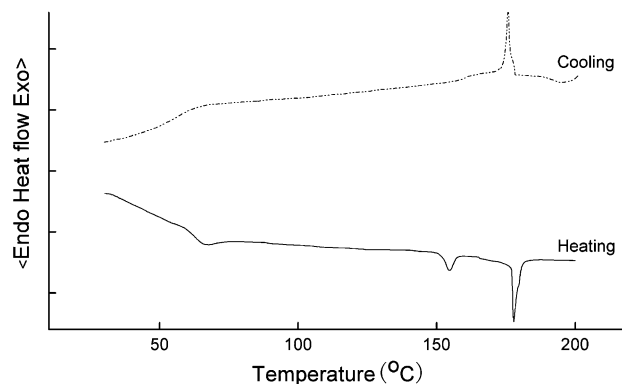


Figure 2. DSC thermograms of OF8T2 for the first cooling (dotted line) and the second heating (solid line) scans recorded at  $10 \text{ }^\circ\text{C} \cdot \text{min}^{-1}$  under nitrogen.

polymeric material with a high PDI.<sup>[16]</sup> The second peak for OF8T2 at 179 °C corresponds to the clearing point ( $T_c$ ), i.e., the transition from the liquid crystal mesophase to the isotropic phase. In the cooling run, however, only one exothermic peak is observed at 179 °C, which is associated with the isotropic-to-liquid crystal phase transition. It is interesting that the recrystallization of OF8T2 in cooling is absent while the recrystallization phenomenon was noted in the case of PF8T2.<sup>[15,16]</sup> To further assess the phase transitions of the oligomer, POM was utilized to observe the morphology evolution with temperature of a OF8T2 film of 10  $\mu\text{m}$  thickness deposited on a glass slide (Figure 3a). When the film was heated to 190 °C at  $10\text{ }^\circ\text{C}\cdot\text{min}^{-1}$ , flaws appeared, which then grew into rod-like crystals about 20  $\mu\text{m}$  long and 3  $\mu\text{m}$  wide (Figure 3b). As the temperature was further increased, the rod-like crystals disappeared, and a Schlieren texture emerged (Figure 3c), and then the film gradually entered an isotropic state (Figure 3d and e). A typical Schlieren texture, as shown in Figure 3, was clearly observed under

crossed polarizers in both heating and cooling processes. Since the Schlieren texture is a distinct feature of nematic liquid crystals, the observations indicate that the liquid crystal phase of OF8T2 is nematic, which is similar to that previously reported for liquid-crystalline PF8T2.<sup>[6,15–17]</sup> On cooling at  $10\text{ }^\circ\text{C}\cdot\text{min}^{-1}$ , the texture remained (Figure 3f), and the recrystallization was almost completely suppressed, which is consistent with the DSC result discussed above that the recrystallization peak was absent in the cooling run. Therefore for OF8T2 oligomer, the liquid crystal texture can be preserved when cooling from melt to generate a liquid-crystalline glass, which is very valuable for better TFT performance because the recrystallization in the cooling process induces carrier trapping at grain boundaries, leading to a reduction in the mobility of the TFT devices.<sup>[19]</sup> In contrast, complete and partial recrystallization occurs for PF8T2 and poly(9,9'-*n*-dioctylfluorene-*alt*-thieno[3,2-*b*]thiophene) (F8TT), respectively in the cooling process at the same cooling rate<sup>[20]</sup>, and for these polymers only through rapid quenching could the characteristic nematic liquid-crystalline texture be frozen to yield liquid-crystalline glasses for high mobility devices.

Nevertheless OF8T2 can still crystallize under suitable conditions. When an OF8T2 film was first heated to 190 °C, which is above its clearing point, and then rapidly cooled to 120 °C and maintained at this temperature for 4 h, the growth of crystals was clearly observed, as shown in Figure 4. Well-connected big spherical crystals of about 300  $\mu\text{m}$  size with pretty patterns were observed under crossed polarizers. Same as the PF8T2 and PF8TT polymers, OF8T2 is a typical  $\pi$ -conjugated hairy-rod molecule. The conjugated stiff backbones tend to aggregate due to the  $\pi$ - $\pi$  interactions, while the two octyl side groups on the fluorene unit increase the steric hindrance between two adjacent OF8T2 chains. The length ratio of the stiff backbone to the octyl side group for OF8T2 is smaller than that for PF8T2 and PF8TT, therefore OF8T2 is more difficult to crystallize than the polymers under the same cooling conditions.

In situ WAXD was then employed to monitor the molecular packing arrangements in the phase transition process. The powder sample was preheated at 190 °C for 10 min, and then rapidly quenched to room temperature

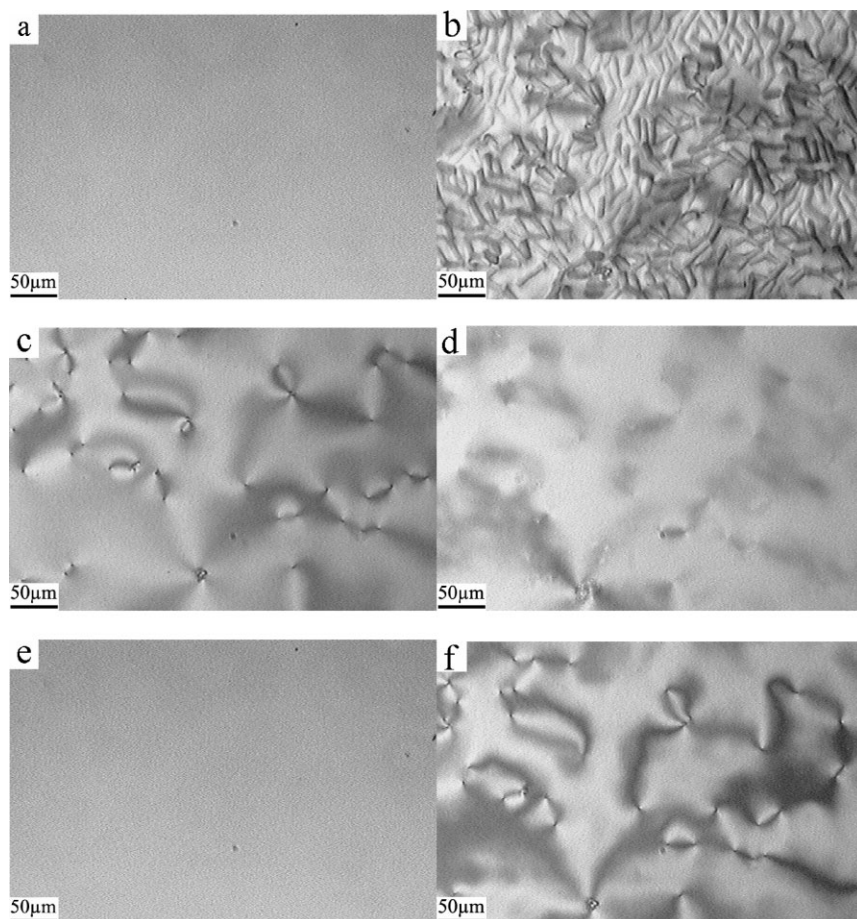


**Figure 3.** POM images through crossed polarizers of an OF8T2 film in the second heating collected at (a) 30.1, (b) 136, (c) 162.0, (d) 171.6, and (e) 180 °C, and upon cooling again to 162 °C (f).

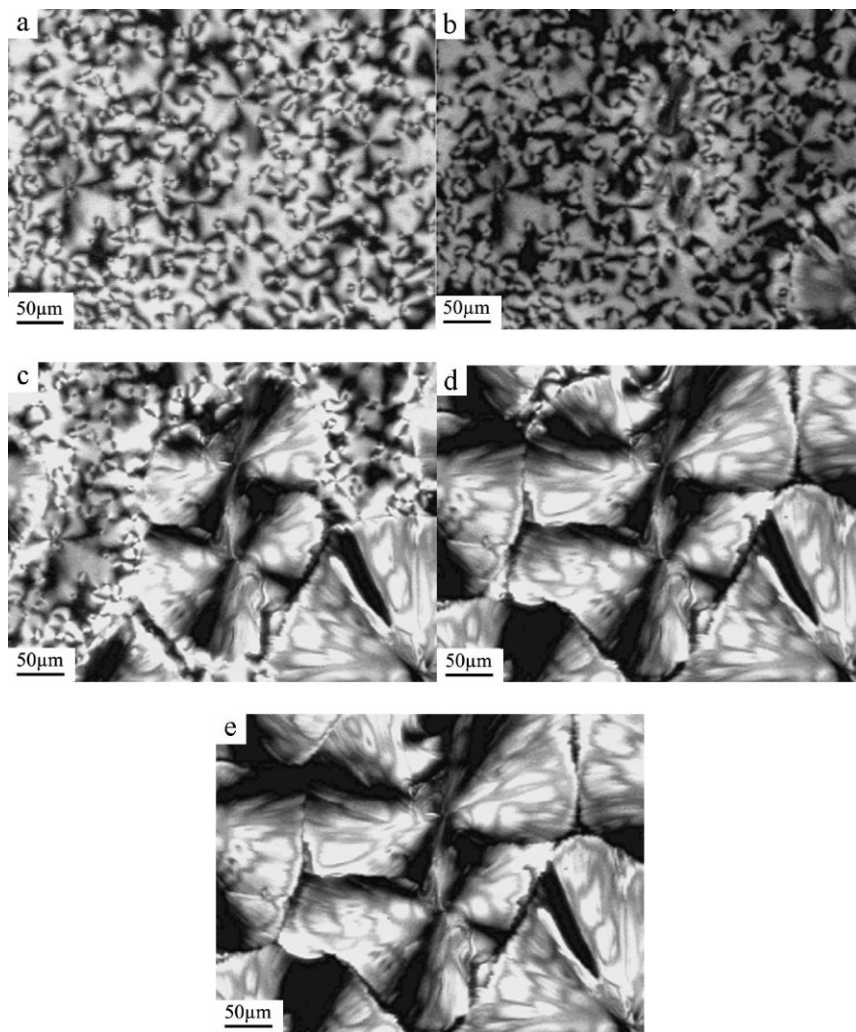


**Figure 4.** POM images through crossed polarizers of an OF8T2 film maintained at 120 °C for (a) 0, (b) 1, (c) 2, (d) 3, and (e) 4 h.

to eliminate the thermal history prior to the experiment. Figure 5 shows a series of the powder WAXD profiles collected at different temperatures. As seen in Figure 5a, from 30 to 90 °C, only a broad peak corresponding to amorphism is observed without any change. Four peaks then appear at 100 °C, and their intensities become stronger with two new peaks at 17.7 and 19.04 ° emerging at 130 °C, indicative of higher crystallinity. At 153 °C all these narrow peaks disappear, and a broad peak at 4.4 Å emerges, which can be assigned to the lateral spacing between the main chains in the nematic phase. The result is consistent with the appearance of the Schlieren texture observed in Figure 3. It can be seen in Figure 5b, that with the temperature further increasing, the peak at 4.4 Å (20.16 °) shifts to 19.1 °, and becomes broader and weaker, suggesting that it enters the isotropic phase and the OF8T2 is in a disordered state. In the cooling process, the

evolution of the WAXD pattern essentially reversed that shown in Figure 5b, i.e., the broad and weak amorphous peak turned into the peak centered at 4.4 Å, and then the nematic liquid crystal phase was maintained all the way to room temperature. The result is also consistent with the DSC observation discussed above that the recrystallization peak was absent in the cooling run.

### Molecular Orientation and Crystallinity in Thin Films

Since semiconducting materials are used mostly as active layers in the form of thin films in organic devices, and molecular orientation has great effect on the device performance; it is necessary to study molecular orientation as well as crystalline structure in these thin films.

The UV-vis spectra of OF8T2 in chloroform solution and in a spin-coated film, respectively are shown in Figure 6. The oligomer solution exhibited an unstructured absorption band at 442 nm, while the absorptions for the oligomer film were at 454 and 482 nm, i.e., the absorption spectrum for the film was better resolved and showed a considerable bathochromic shift, suggesting that the molecules adopted a more extended conformation in the solid state.<sup>[18]</sup> Therefore, the

oligomer molecules may have a tendency to form ordered structures in the films, and it was investigated with WAXD.

The thin film on a silicon wafer exhibited no diffraction peaks (Figure 7a), suggesting the absence of any crystalline structure, which is consistent with the literature report that chains are randomly oriented in spin-cast films.<sup>[21]</sup> Upon annealing, the randomly oriented molecules began to reorganize. When the film was annealed at 105 °C for 1 h, sharp diffraction peaks were observed at 5.22, 10.44, 15.67, and 20.90 ° (Figure 7a), corresponding to the first-, second-, third-, and fourth-order diffractions, respectively, arising from the layering distance between sheets of the main chains separated by the octyl groups orienting normal to the substrate (Figure 7b).<sup>[15,22]</sup> In contrast, when the OF8T2 powder was annealed in the same way, the number of diffraction peaks increased from two to eleven

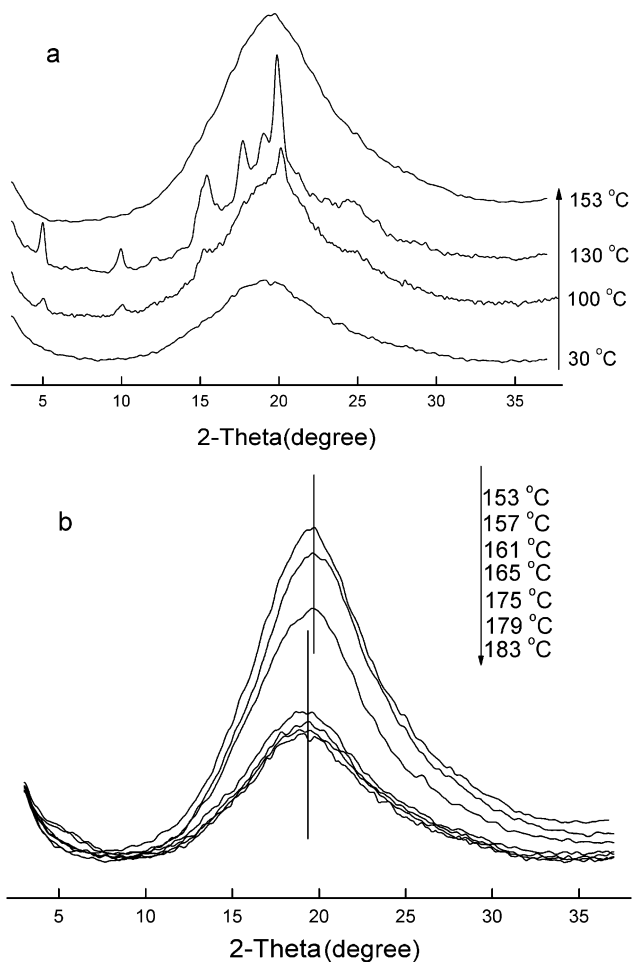


**Figure 5.** Temperature-resolved powder WAXD profiles of OF8T2 at given temperatures in the heating process: (a) from 30 to 153 °C, and (b) from 153 to 183 °C.

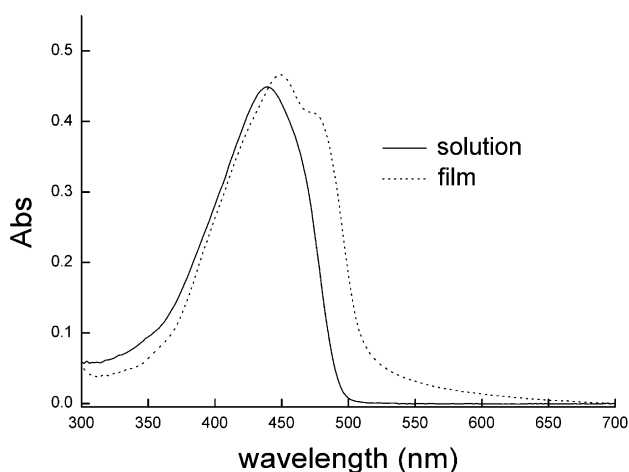


**Figure 6.** UV-vis spectra of an OF8T2 solution in chloroform (solid line) and a spin-coated OF8T2 film (dotted line).

(Figure 7a). The presence of only one set of diffraction and the absence of other diffractions observed for the bulk manifests the formation of ordered layer structure in the thin film. It has been reported that spin-coating process results in chains lying in the film,<sup>[22]</sup> and molecular motions are limited due to the spatial suppression and surface suppression in thin films.<sup>[23]</sup> Without any specific interactions at the ends of the OF8T2 chains, the standing up of the stiff molecules on their ends is very unlikely. As a result, in thin films the OF8T2 molecules arrange with the plane of conjugation being normal to the substrate, which is expected to yield excellent TFT properties.

The OF8T2 thin films spin-coated on various other substrates, including glass plates, quartz plates, and Au substrates all exhibited the same structure, indicating that the OF8T2 oligomer has an intrinsic tendency to assume such an aligned structure upon annealing in thin films.<sup>[24]</sup>

It has been reported that the orientation of molecular chains and lamellar crystals in thin films depends on the film thickness.<sup>[25]</sup> To assess the thickness effect on the

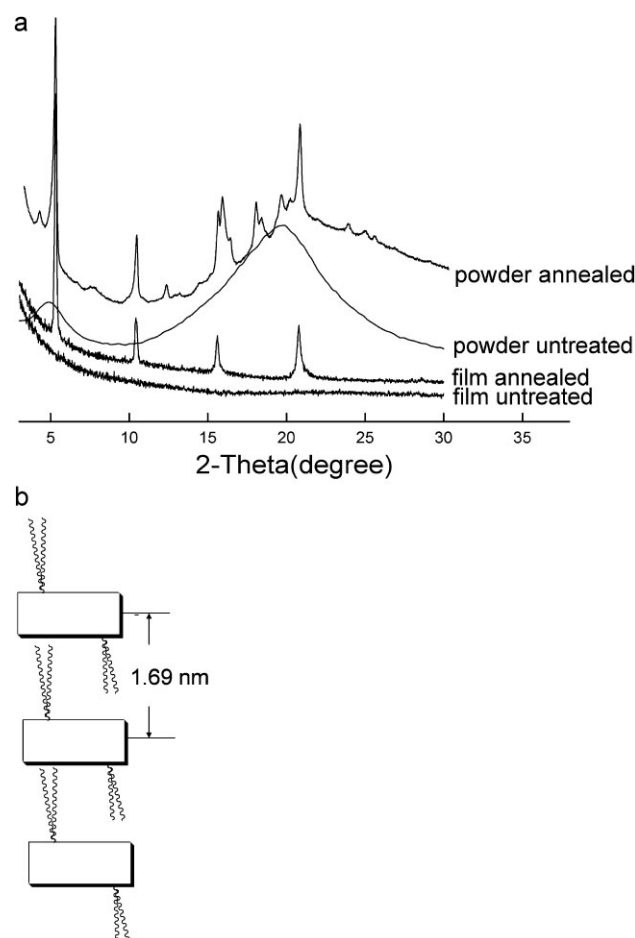


**Figure 7.** (a) WAXD profiles of various OF8T2 samples, where the annealing was done at 105 °C for 1 h. (b) Schematic representation of the ordered structure in the films.

OF8T2 molecules, thin films of different thicknesses were prepared by conventional spin-coating. All the films were continuous and smooth, and a typical example of the spin-coated thin film is shown in Figure 8b. The films were annealed at 105 °C and their WAXD patterns were recorded (Figure 8a). For the film of 20 nm thickness, no diffraction peak was observed. A typical AFM height image of the 20 nm thin film is shown in Figure 8c, and dewetting of the film is clearly seen, which explains why crystallinity was absent in the OF8T2 film of 20 nm thickness. For the films of 40 nm and thicker, WAXD profiles showed same four peaks as discussed above in Figure 7, and the peaks became sharper as the thickness of the film increased. Actually crystalline grain size can be calculated using the Scherrer formula<sup>[26]</sup>

$$D = \frac{K\lambda}{\beta \cos \theta}$$

where  $D$  is the crystal size,  $K$  the constant which depends on both the apparatus and the sample studied ( $K=0.89$ ),  $\beta$  is the full width at half maximum of the peak, and  $\lambda = 1.5406 \text{ \AA}$  (Cu  $K_{\alpha}$  radiation). The crystalline grain size in the film calculated based on the (100) diffraction decreased from 71.3 nm in the 80-nm film to 33.2 nm in the 40-nm film. In addition, as shown in Figure 8d and e, AFM topographic images indicate that the crystalline domains in the 80-nm film larger in the lateral directions than that in the 40-nm film.

Temperature is another determinative complication which affects crystallization in addition to film thickness, which was studied using in situ WAXD (Figure 9). No peaks appeared from room temperature to 90 °C. As the temperature increased to 100 °C, sharp diffraction peaks were observed at 5.22, 10.44, 15.67, and 20.90 ° attributed to the layering distance between sheets of the main chains, as discussed above for Figure 7. The peak intensities increased greatly to reach the maxima at 120 °C, and then began to decrease as

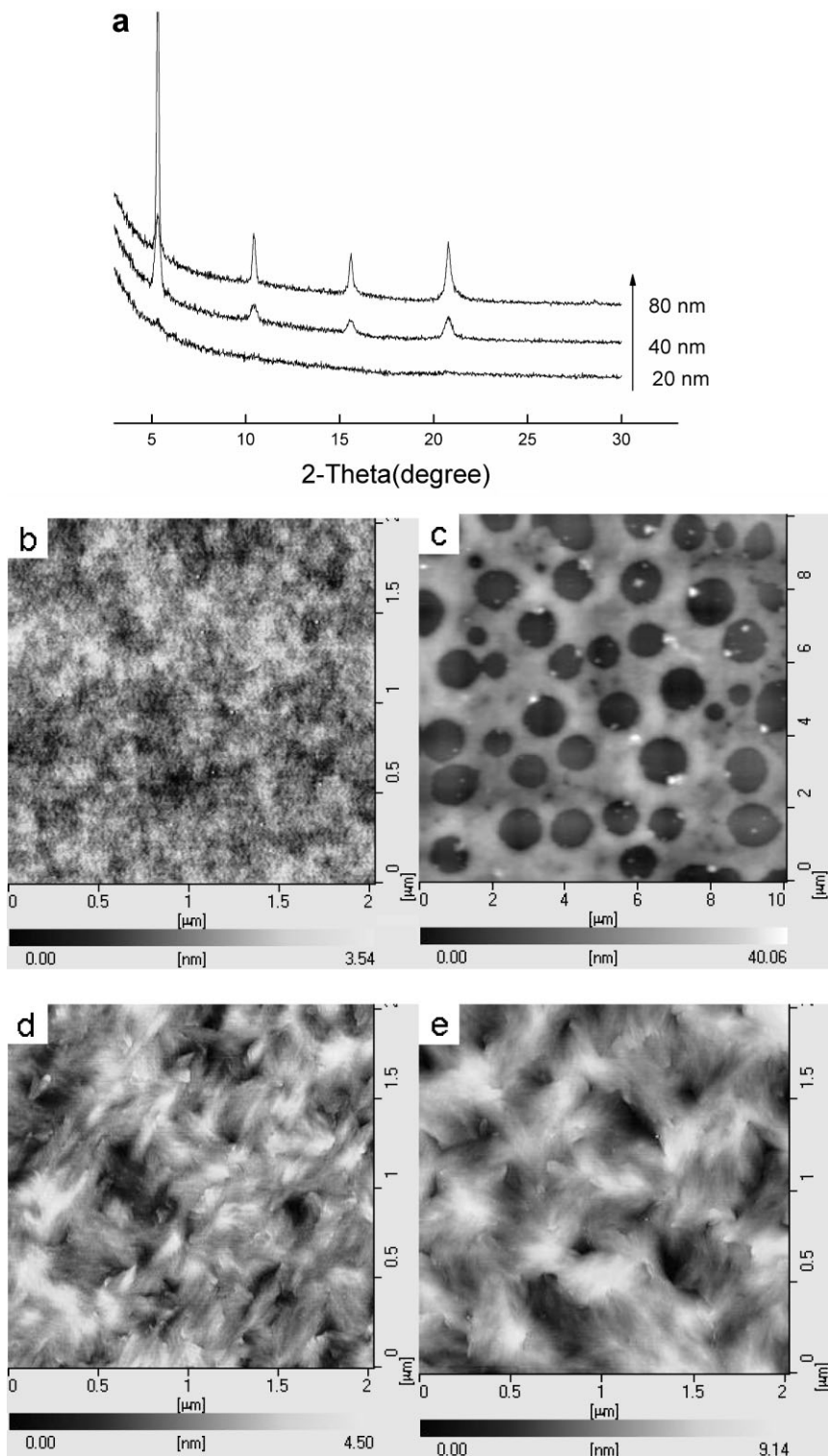


**Figure 8.** (a) WAXD profiles of OF8T2 films of different thicknesses annealed at 105 °C. AFM topographic images of (b) a spin-cast OF8T2 film, and films annealed at 105 °C with the thickness of (c) 20, (d) 40, and (e) 80 nm.

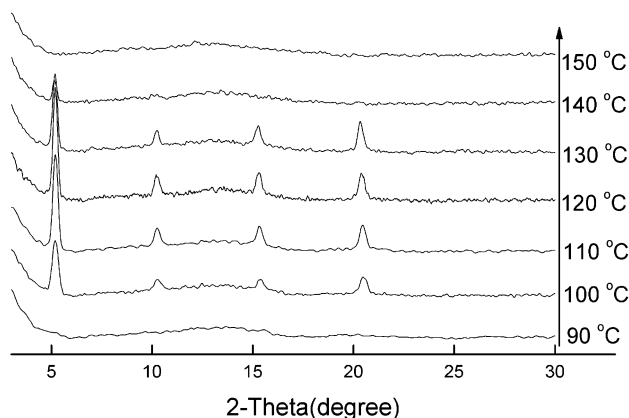


Figure 9. Temperature-resolved WAXD profiles of an OF8T2 film of  $\approx 40$  nm thickness in the heating process.

the temperature further increased. At 140 °C, only the peak at 5.22°, i.e., the first-order diffraction, remained, which subsequently disappeared when the temperature reached 150 °C. It is worth notice that during the whole heating process, other diffractions observed for the bulk sample never showed up, apparently, a result of preferred orientation of the crystals due to the spatial suppression and surface suppression in thin films.<sup>[23]</sup>

Molecular alignment has proved to be important in many device applications. The properties of oriented materials such as stiffness and charge transport can be increased by orders of magnitude. Self-aligning nature of liquid crystals provides an effective way to the fabrication of oriented thin films. It is well-known that the spin-coating process results in the flexible polymer chains randomly oriented within the film because of the formation of the entanglement network on the substrate. For rigid-rod polymers, only a small number of the chains are aligned or partially aligned to the radial direction.<sup>[22]</sup> To align the  $\pi$ -conjugated hairy-rod OF8T2 molecules, the oligomer was deposited on a rubbed polyimide surface and then annealed in the liquid crystal phase for 5 min. The degree of alignment was then estimated by polarized UV-vis absorption spectroscopy. The polarized absorption of the rubbed polyimide film was measured before the OF8T2 film was deposited as the background, and was subtracted from the absorbance of the sample. The polarized UV-vis spectra are shown in Figure 10. It can be seen that the absorption maxima appear at 450 and 487 nm, which are in the spectral region of  $\pi$ - $\pi^*$  transition.<sup>[16]</sup> The dichroic ratio ( $R = A_{\parallel}/A_{\perp}$ ) for light polarized parallel versus perpendicular to the rubbing direction is about 5.5, which reflects that the transition dipole moment, the same as the chain direction for the OF8T2 molecule, oriented predominantly parallel to the rubbing direction. When the OF8T2 was deposited on the rubbed polyimide substrate,

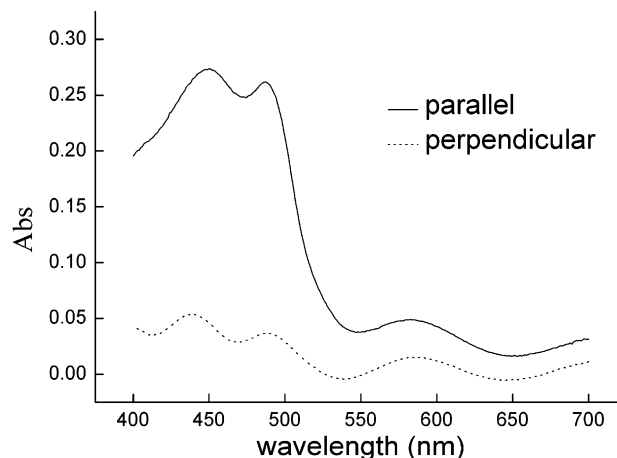


Figure 10. Polarized UV-vis absorption spectra of an OF8T2 thin film deposited on a rubbed polyimide surface parallel (solid line) and perpendicular (dotted line) to the rubbing direction, respectively.

the OF8T2 molecules close to the interface aligned their long axes along the rubbing direction, and the interactions between neighboring OF8T2 molecules induced the underlying molecules to align along the same direction. Long-range alignment order can thus be obtained, which is helpful for improving the mobility of the field-effect transistors.

## Conclusion

The OF8T2 oligomer has good solubility and stability, which afford the possibility for making solution-processable devices. The oligomer exhibits a nematic thermotropic liquid crystal phase, and a phase transition between the crystalline and the nematic liquid-crystalline states. When cooling from melt, the liquid crystal texture can be easily preserved to generate liquid-crystalline glass, which is very valuable for better mobility of organic devices. In thin films with thickness of 40 nm and above, the conjugated oligomer molecules form ordered lamellar structure with the plane of conjugation being normal to the substrate, which is advantageous for yielding excellent TFT properties. Both film thickness and annealing temperature affect the morphology and molecular orientation in OF8T2 films. In addition, unidirectional alignment of the molecules can be induced by depositing OF8T2 on rubbed polyimide surfaces and then annealing in the liquid crystal phase. These results suggest that OF8T2 is a promising material for the active layer in organic devices, and this work may help the fabrication of ordered thin films for use in organic devices to improve their performance.

Acknowledgements: This work was supported by the *National Natural Science Foundation of China* (20423003, 20774097). Z. S. thanks the *NSFC Fund for Creative Research Groups* (50621302) for support.

Received: March 29, 2008; Revised: May 12, 2008; Accepted: May 13, 2008; DOI: 10.1002/macp.200800167

Keywords: liquid crystals; orientation; oligomers; phase transitions; thin films

- [1] G. Horowitz, *Adv. Mater.* **1998**, *10*, 365.
- [2] N. Kiriy, V. Bocharova, A. Kiriy, M. Stamm, F. C. Krebs, H. J. Adler, *Chem. Mater.* **2004**, *16*, 4765.
- [3] J. Locklin, D. W. Li, S. C. B. Mannsfeld, E. J. Borkent, H. Meng, R. Advincula, Z. Bao, *Chem. Mater.* **2005**, *17*, 3366.
- [4] T. Erb, U. Zhokhavets, G. Gobsch, S. Raleva, B. Stuhn, P. Schilinsky, C. Waldauf, C. J. Brabec, *Adv. Funct. Mater.* **2005**, *15*, 1193.
- [5] Y. H. Geng, A. C. A. Chen, J. J. Ou, S. H. Chen, K. Klubek, K. M. Vaeth, C. W. Tang, *Chem. Mater.* **2003**, *15*, 4352.
- [6] E. Lim, B. J. Jung, H. K. Shim, *Macromolecules* **2003**, *36*, 4288.
- [7] B. Liu, Y. H. Niu, W. L. Yu, Y. Cao, *Synth. Meth.* **2002**, *129*, 129.
- [8] G. Vamvounis, G. L. Schulz, S. Holdcroft, *Macromolecules* **2004**, *37*, 8897.
- [9] T. A. Chen, X. M. Wu, R. D. Rieke, *J. Am. Chem. Soc.* **1995**, *117*, 233.
- [10] R. D. McCullough, S. Tristramnagle, S. P. Williams, R. D. Lowe, M. Jayaraman, *J. Am. Chem. Soc.* **1993**, *115*, 4910.
- [11] T. J. Prosa, M. J. Winokur, J. Moulton, P. Smith, A. J. Heeger, *Macromolecules* **1992**, *25*, 4364.
- [12] H. Sirringhaus, P. J. Brown, R. H. Friend, M. M. Nielsen, K. Bechgaard, B. M. W. Langeveld-Voss, A. J. H. Spiering, R. A. J. Janssen, E. W. Meijer, P. Herwig, D. M. de Leeuw, *Nature* **1999**, *401*, 685.
- [13] G. M. Wang, J. Swensen, D. Moses, A. J. Heeger, *J. Appl. Phys.* **2003**, *93*, 6137.
- [14] M. Grell, D. D. C. Bradley, G. Ungar, J. Hill, K. S. Whitehead, *Macromolecules* **1999**, *32*, 5810.
- [15] L. Kinder, J. Kanicki, P. Petroff, *Synth. Met.* **2004**, *146*, 181.
- [16] L. R. Pattison, A. Hexemer, E. J. Kramer, S. Krishnan, P. M. Petroff, D. A. Fischer, *Macromolecules* **2006**, *39*, 2225.
- [17] H. Sirringhaus, R. J. Wilson, R. H. Friend, M. Inbasekaran, W. Wu, E. P. Woo, M. Grell, D. D. C. Bradley, *Appl. Phys. Lett.* **2000**, *77*, 406.
- [18] X. J. Zhang, Y. Qu, L. J. Bu, H. K. Tian, J. P. Zhang, L. X. Wang, Y. H. Geng, F. S. Wang, *Chem. Eur. J.* **2007**, *13*, 6238.
- [19] M. Redecker, D. D. C. Bradley, M. Inbasekaran, E. P. Woo, *Appl. Phys. Lett.* **1999**, *74*, 1400.
- [20] E. Lim, B. J. Jung, J. Lee, H. K. Shim, J. I. Lee, Y. S. Yang, L. M. Do, *Macromolecules* **2005**, *38*, 4531.
- [21] D. McBranch, I. H. Campbell, D. L. Smith, J. P. Ferraris, *Appl. Phys. Lett.* **1995**, *66*, 1175.
- [22] C. W. Y. Law, K. S. Wong, Z. Yang, L. E. Horsburgh, A. P. Monkman, *Appl. Phys. Lett.* **2000**, *76*, 1416.
- [23] Y. Kikkawa, H. Abe, M. Fujita, T. Iwata, Y. Inoue, Y. Doi, *Macromol. Chem. Phys.* **2003**, *204*, 1822.
- [24] T. Yamamoto, H. Kokubo, T. Morikita, *J. Polym. Sci. Part B Polym. Phys.* **2001**, *39*, 1713.
- [25] Z. J. Hu, H. Y. Huang, F. J. Zhang, B. Y. Du, T. B. He, *Langmuir* **2004**, *20*, 3271.
- [26] B. D. Cullity, "Elements of X-ray Diffraction", 2<sup>nd</sup> edition, Addison-Wesley, Reading, MA 1978.